

Article

Ionic Strength of Methylcellulose-Based Films: An Alternative for Modulating Mechanical Performance and Hydrophobicity for Potential Food Packaging Application

Rafael Resende Assis Silva ^{1,*}, Clara Suprani Marques ², Tarsila Rodrigues Arruda ², Samiris Cocco Teixeira ², Taíla Veloso de Oliveira ², Paulo Cesar Stringheta ², Ana Clarissa dos Santos Pires ² and Nilda de Fátima Ferreira Soares ²

¹ Department of Materials Science and Engineering, Federal University of São Carlos, São Carlos 13565-905, Brazil

² Food Technology Department, Federal University of Viçosa, Viçosa 36570-900, Brazil; supraniclara@gmail.com (C.S.M.); tarsila.arruda@ufv.br (T.R.A.); samiristeixeira@gmail.com (S.C.T.); taíla.oliveira@ufv.br (T.V.d.O.); stringap@ufv.br (P.C.S.); ana.pires@ufv.br (A.C.d.S.P.); nfsoares10@gmail.com (N.d.F.F.S.)

* Correspondence: rafaelras@estudante.ufscar.br; Tel.: +55-(37)-99131-3471



Citation: Silva, R.R.A.; Marques, C.S.; Arruda, T.R.; Teixeira, S.C.; de Oliveira, T.V.; Stringheta, P.C.; dos Santos Pires, A.C.; de Fátima Ferreira Soares, N. Ionic Strength of Methylcellulose-Based Films: An Alternative for Modulating Mechanical Performance and Hydrophobicity for Potential Food Packaging Application. *Polysaccharides* **2022**, *3*, 426–440. <https://doi.org/10.3390/polysaccharides3020026>

Academic Editor: Rajkumar Patel

Received: 17 March 2022

Accepted: 9 May 2022

Published: 20 May 2022

Publisher's Note: MDPI stays neutral with regard to jurisdictional claims in published maps and institutional affiliations.



Copyright: © 2022 by the authors. Licensee MDPI, Basel, Switzerland. This article is an open access article distributed under the terms and conditions of the Creative Commons Attribution (CC BY) license (<https://creativecommons.org/licenses/by/4.0/>).

Abstract: The growing environmental concern with the inappropriate disposal of conventional plastics has driven the development of eco-friendly food packaging. However, the intrinsic characteristics of polymers of a renewable origin, e.g., poor mechanical properties, continue to render their practical application difficult. For this, the present work studied the influence of ionic strength (IS) from 0 to 500 mM to modulate the physicochemical properties of methylcellulose (MC). Moreover, for protection against biological risks, Nisin-Z was incorporated into MC's polymeric matrices, providing an active function. The incorporation of salts (LiCl and MgCl₂) promoted an increase in the equilibrium moisture content in the polymer matrix, which in turn acted as a plasticizing agent. In this way, films with a hydrophobic surface (98°), high true strain (85%), and low stiffness (1.6 mPa) can be manufactured by addition of salts, modulating the IS to 500 mM. Furthermore, films with an IS of 500 mM, established with LiCl, catalyzed antibacterial activity against *E. coli*, conferring synergism and extending protection against biological hazards. Therefore, we demonstrated that the IS control of MC dispersion presents a new alternative to achieve films with the synergism of antibacterial activity against Gram-negative bacteria in addition to flexibility, elasticity, and hydrophobicity required in various applications in food packaging.

Keywords: ionic strength; food packaging; active films; antibacterial activity; plasticizing effect; methylcellulose; strain true; performance mechanical

1. Introduction

Bio-based polymers have been widely studied as potential food packaging materials to replace, totally or in part, petroleum-based plastics [1–7]. However, certain features, such as higher gas/water vapor permeability, poorer UV–Vis barrier, higher costs of production, poorer mechanical properties, and higher hydrophilicity, still hinder or prevent their practical application [4,6]. In order to improve these properties and bring them closer to the those exhibited by conventional plastics, many strategies are proposed: chemical or physical modification, incorporation of additives with particular properties, such as plasticizers and nanoparticles fillers, blends of two or more polymers, and optimization of the sample preparation method [1,6,8,9].

The modulation of ionic strength (IS) through the incorporation of salts is a scarcely studied approach that appears promising regarding material enhancement. For example, by adding divalent salts into polymeric matrices, Silva et al. [3] manufactured highly flexible

methylcellulose (MC) films, producing a material with enhanced functionality. Flexibility, for instance, is a crucial parameter that must be accounted for when selecting the packaging material since non-flexible and brittle materials, such as bio-based plastics, may not be able to maintain their physical integrity during handling [10]. Therefore, the increase of bio-based film flexibility is an essential step in the ongoing search for the successful implementation of these polymers as food packaging materials.

In addition to the impact parameters of films, modulation by IS can also influence the kinetics diffusion of certain substances and their antimicrobial properties, as shown by Wang et al. [11]. In order to mitigate food loss due to antimicrobial contamination, the incorporation of active compounds into polymeric matrices to develop active packaging is widely studied as a complementary technology to assist in food preservation [12–16]. Among the substances that can be added into polymeric matrices, it is worth highlighting nisin, an antimicrobial peptide approved as a food preservative in more than 50 countries and widely used in dairy products to extend their shelf-life and ensure food safety [7,17,18]. Nisin-Z is a commercial type of nisin that presents high activity against a wide range of Gram-positive bacteria and low or no effectiveness against Gram-negative bacteria [18]. Kuwano et al. [11] verified that the low activity of Nisin-Z against *Escherichia coli*, a Gram-negative bacterium, decreased when NaCl concentration increased. However, different salts can cause different physicochemical and antimicrobial effects; in other words, each case must be assessed separately since changes observed in Nisin-Z vary according to the nature of the salt [18].

In this context, the present work aimed to develop and investigate changes in MC-based films when incorporated with Nisin-Z and different concentrations of a monovalent salt (LiCl) or a divalent salt ($MgCl_2$). The influence of IS effects and the ions' electric charge (EC) on the films' mechanical properties, water vapor barrier, light barrier, and thermal properties was evaluated. Moreover, we investigated whether the IS would promote changes in the hydrophilic nature of the polymer, as well as the possible synergistic effect on the antibacterial property of the active films when evaluated against three microorganisms: *E. coli*, *Staphylococcus aureus* and *Lactobacillus plantarum*.

2. Materials and Methods

2.1. Materials

Lithium chloride (LiCl) was acquired from Vetec Co. (Duque de Caxias, RJ, Brazil). Ethanol was purchased from Neon Co. (Suzano, SP, Brazil). Magnesium chloride ($MgCl_2$) and glycerol were acquired from Synth Co. (Diadema, SP, Brazil). Methylcellulose (40,000 M_n , viscosity 400 cP, 1.6 to 1.9 Degree of Substitution) was purchased from Sigma-Aldrich Co. (St. Louis, MO, USA). Nisin-Z was acquired from Handary (Evere, Brussels, Belgium). Sodium chloride (NaCl) was purchased from Fmaia (Belo Horizonte, Brazil). *S. aureus* ATCC 6538, *L. plantarum* ATCC 8014, (Gram-positive) and *E. coli* ATCC 11,229 (Gram-negative) were acquired from culture stock at Packaging Laboratory, Food Technology Laboratory, Viçosa, Federal University of Viçosa.

2.2. Methods

Production of MC-Based Films and Active Films

The films with different IS were prepared using the casting method described by Silva et al. [3] with modifications. Salts solutions 25, 50, 250, and 500 millimolar of LiCl or $MgCl_2$ in 50 mL of deionized water were added in a beaker and heated to $100\text{ }^\circ\text{C} \pm 2\text{ }^\circ\text{C}$. The salts concentrations were calculated employing Equation (1). Then, 1 g of MC polymer was dispersed in this solution under magnetic stirring at 600 rpm for 15 min. Next, glycerol (0.2 g) was added to the polymer dissolution and stirred for 10 min. When the temperature was reduced to $40\text{ }^\circ\text{C}$, Nisin-Z at 10% wt. of MC was added into the dispersion, with pH = 6.5, to evaluate the antibacterial activity synergy with the salts. Thereby, the film-forming solutions were poured onto glass plates (34 cm \times 18.5 cm) and placed in a conditional chamber for 48 h at $23 \pm 2\text{ }^\circ\text{C}$ and relative humidity (RH) of 55% for solvent

evaporation. Following this, the films were removed from the glass plate with the aid of a spatula. The variation of the thickness of the films was studied due to the variation of the IS, since the same mass of MC was added for all treatments. The uniformity of the films was controlled by the leveling of the base of the conditional chamber. The control was prepared under the same conditions without chloride salt (0 mM).

$$FI = \mu = \frac{\sum_{i=1}^n Z_i^2 * C_i}{2} \quad (1)$$

where μ is the IS ($\text{mol}\cdot\text{L}^{-1}$), C_i is the concentration of the ion (i) ($\text{mol}\cdot\text{L}^{-1}$), Z_i is the number of the EC of the ion (i).

2.3. Film Characterization

2.3.1. Fourier Transform Infrared Spectroscopy (FTIR)

The FTIR spectra of the treatments were obtained using an FTIR spectrometer, model Nicolet 6700 (Thermo Scientific, Waltham, MA, USA), equipped with an Attenuated Total Reflectance (ATR), from 4000 to 900 cm^{-1} , at a spectral resolution of 2 cm^{-1} and 32 scans per sample.

2.3.2. Energy Dispersive Spectroscopy (EDS)

A scanning electron microscope (JEOL JSM-6010LA) equipped with an energy dispersive spectroscopy (EDS) system was used, with 1000 \times magnification at an accelerating voltage of 5 kV to obtain images of the active films and controls in order to confirm the presence and dispersion of Nisin-Z into the polymer matrix.

2.3.3. Thermogravimetry (TG)

The thermogravimetric curves of MC-based films were constructed in DTG thermal analyzer (SHIMADZU, model 60H, Kyoto, Japan) to evaluate the films' thermal stability. Approximately 3 mg of each film was packaged in alumina pans and heated from 30 $^{\circ}\text{C}$ to 600 $^{\circ}\text{C}$ at a rate of 10 $^{\circ}\text{C}\cdot\text{min}^{-1}$, under 50 $\text{mL}\cdot\text{min}^{-1}$ nitrogen flow rate.

2.3.4. Contact Angle

The contact angle between water and film surface (solvent-evaporation side) was determined using a goniometer (Kruss, Hamburg, Germany), employing the sessile drop method. The analysis was performed at 25 $^{\circ}\text{C} \pm 2^{\circ}\text{C}$ with three repetitions for each treatment.

2.3.5. Light Barrier Property and Moisture Content of Films

The light transmittance of the MC-based films was evaluated using a UV-Vis Spectrophotometer (model UV 1800, Shimadzu, Kyoto, Japan), operating from 200 to 800 nm. Samples with 3 g of MC-based films were dried (105 $^{\circ}\text{C}$ for 24 h), and by weight difference, the moisture content was determined, according to the ASTM D644-99 methodology [19]. A total of seven measurements were accomplished for each determination.

2.3.6. Density, Thickness, and Mechanical Performance

MC-based film thickness was determined using a digital micrometer with an accuracy of 0.001 mm (Mitutoyo Corporation, Kawasaki, Japan). The averaging of 10 random measurements determined the final thickness within the film's area. Film density was calculated by the quotient of sample weight over sample volume. Mechanical performance of the MC-based films was determined using a Universal Testing Machine, model 3367 (Instron Corporation, Norwood, MA, USA) equipped with a 0.5 kN load cell, in accordance with the standard method ASTM D882-12 [20]. Samples were previously conditioned for 48 h at 23 $^{\circ}\text{C} \pm 2^{\circ}\text{C}$ and 50% $\pm 3\%$ of relative humidity (RH). MC-based films were shaped into rectangular specimens (150 \times 25 mm^2), grabbed by two grips initially separated by 100 mm, and stretched at a crosshead speed of 50 $\text{mm}\cdot\text{min}^{-1}$. The tensile strength-

σ_{max} (MPa), modulus of elasticity– E (MPa), true strain– ε_t (%), and linear strain– ε_l (%) properties were determined using Equations (2)–(5) respectively. The tests were carried out with at least seven replications.

$$\sigma_{max} = \frac{F}{A_0} \quad (2)$$

$$E = \frac{\sigma_{max}}{\frac{\Delta l}{l_0}} \quad (3)$$

$$\varepsilon_t = \ln\left(\frac{l_f}{l_0}\right) \times 100 \quad (4)$$

$$\varepsilon_l = \frac{\Delta l}{l_0} \times 100 \quad (5)$$

where (F) is the maximum force supported, (A_0) is the initial cross-sectional area of the specimen, (l_f) is the distance between the grips at the moment of rupture, (l_0) is the initial length of the specimen, and (Δl) is the variation between l_f and l_0 .

2.3.7. Water Vapor Permeability (WVP)

The WVP of the MC-based films was determined gravimetrically according to ASTM method E96-95 with modifications [1,21]. Before the analysis, the samples were conditioned at $25\text{ }^\circ\text{C} \pm 2\text{ }^\circ\text{C}$ and 53% RH for 12 h. The films were sized 80 mm in diameter, placed under circular paraffin capsules, and sealed with liquid paraffin. Capsules were filled with MgCl_2 saturated solution (32.5% RH) and stored at $25\text{ }^\circ\text{C} \pm 2\text{ }^\circ\text{C}$ in a desiccator containing a saturated solution of NaCl to maintain a RH of 75%. Samples were weighed every 2 h for 48 h, and WVP was calculated using three replicates and expressed in ($\text{g}\cdot\mu\text{m}\cdot\text{m}^{-2}\cdot\text{day}^{-1}\cdot\text{kPa}^{-1}$).

2.3.8. Antibacterial Activity

The antibacterial effect of the manufactured films was investigated against *S. aureus* ATCC 6538, *L. plantarum* ATCC 8014 (Gram-positive) and *E. coli* ATCC 11,229 (Gram-negative). The cultures were obtained from the culture collection of the Packaging Laboratory, Federal University of Viçosa, Viçosa, MG, Brazil. For inoculum preparation, the bacteria were activated on brain heart infusion (BHI, Kasvi, Roseto degli Abruzzi, Italy) broth, incubated at $37\text{ }^\circ\text{C} \pm 1\text{ }^\circ\text{C}$ for 24 h, streaked over non-selective agar (PCA, Oxoid, Basingstoke, Hampshire, UK), and incubated at $37\text{ }^\circ\text{C} \pm 1\text{ }^\circ\text{C}$ for 24 h (*E. coli* and *S. aureus*) or 48 h in anaerobiosis (*L. plantarum*). Selected colonies of each bacterium were taken from the agar and suspended in 0.85% (*wt/v*) saline solution until obtaining suspensions with a density similar to 0.5 McFarland turbidity standard (approximately $1\text{--}2 \times 10^8\text{ CFU}\cdot\text{mL}^{-1}$) [22]. Subsequently, the prepared bacterial suspensions were spread on the surface of solidified BHI agar plate with a swab, and circular samples of the films ($\varnothing = 1\text{ cm}$) were placed on the agar. The Petri dishes were incubated for 24 h at $37\text{ }^\circ\text{C} \pm 1$ (*E. coli* and *S. aureus*) or 48 h at $37\text{ }^\circ\text{C} \pm 1$ in anaerobiosis (*L. plantarum*), and the resulting inhibition zones were measured (mm) [12].

2.4. Statistical Analysis

Experiments were carried out following a completely randomized design with two factors: EC, with two levels (monovalent EC for lithium and divalent EC for magnesium) and IS, with five levels (0, 25, 50, 250, and 500 mM of LiCl or MgCl_2). All analyses and measurements were performed three times, and the difference was determined, considering the confidence level of 95%. All statistical analyses were performed with Origin Pro 8.5 and Minitab statistical program, version 17.

3. Results

3.1. FTIR, EDS, and Contact Angle

Changes in the FTIR absorption behavior allow us to infer the intra and intermolecular interactions of the components present in the films (glycerol, MC, water, and chlorinated salts) as a function of the EC of the salts and the IS of the system when incorporating LiCl and MgCl₂ (Figure 1). Four main peaks or bands are highlighted in Figure 1. The band at 3400 cm⁻¹ refers to the stretching of the OH bond, and it was found that the increase in IS in the films containing salts increased the band intensity and shifted to shorter wavelengths [23,24]. The shift of this band to shorter wavelengths is justified by intermolecular interactions of the ion-dipole type between the hydroxyl groups of methylcellulose and counter-ions of the dissociated salts, weakening the O-H covalent bond and reducing the absorption frequency [3].

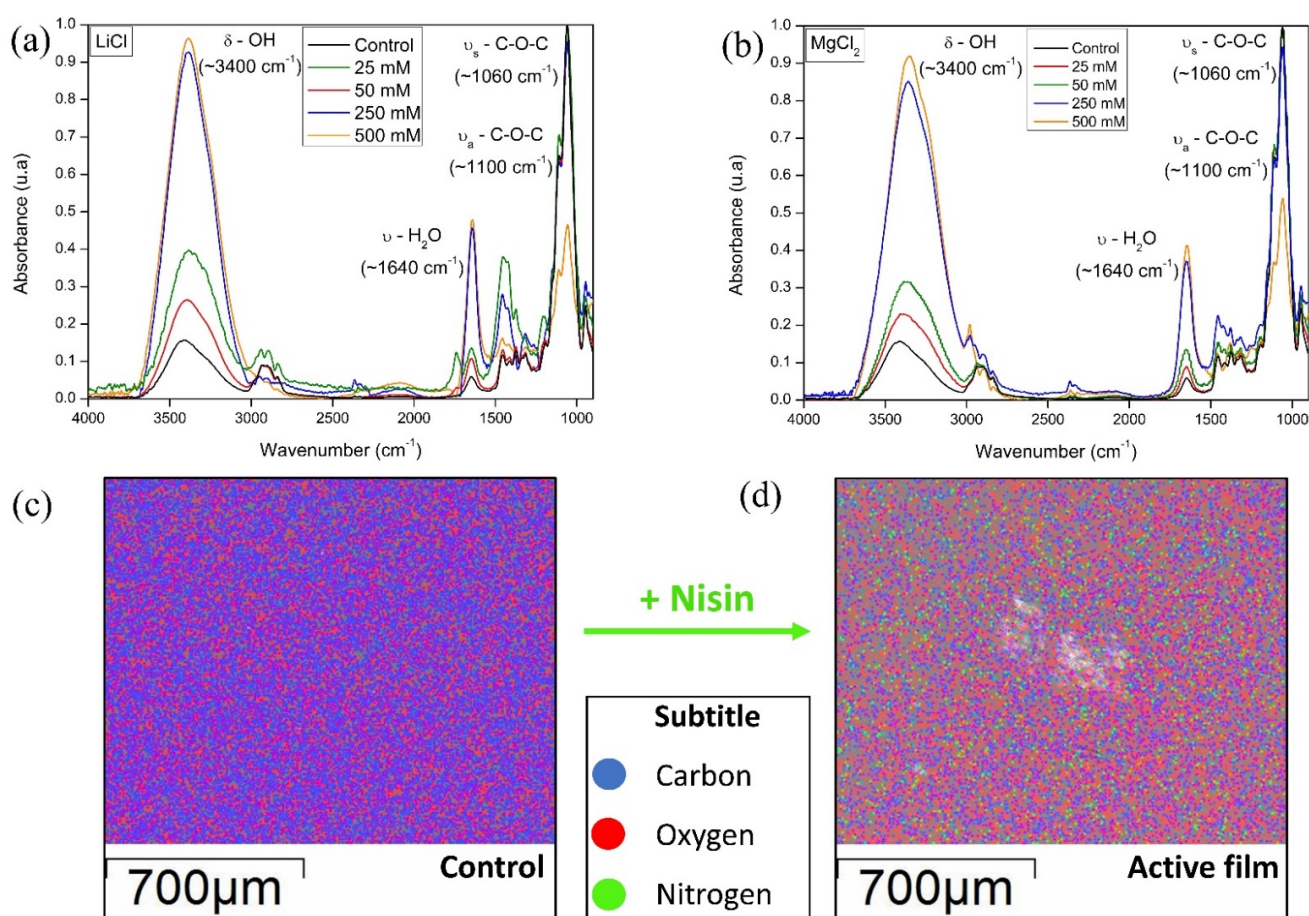


Figure 1. FTIR spectra of MC-based films with 0, 25, 50, 250, and 500 mM due to LiCl (a) or MgCl₂ addition (b), and the EDS full elemental maps of (c) control film (0 mM of IS) and (d) active film (0 mM of IS) incorporated with Nisin-Z.

Furthermore, we confirmed that the IS increase of the polymeric dispersion produced MC films with significantly higher peak intensity at 1637 cm⁻¹, referring to the angular deformation of the water [3,24]. In turn, the difference in the EC of the cations did not significantly influence the water absorption capacity. The absence of chemical reactions in the polymer structure is confirmed by the visualization of MC characteristic peaks in the 1270–1030 cm⁻¹ range, associated with asymmetric stretching bands of ethers, and symmetrical stretching of ethers at 1180–1050 cm⁻¹ [24,25].

Meanwhile, the wavelengths from 1320 to 1450 cm⁻¹ are associated with the harmonic peaks of the ether group and the angular deformation of C-H of alkanes present in the

MC [24]. The other peaks present in the infrared spectrum will not show significant changes under the effect of the treatments evaluated and, therefore, were used only to diagnose the presence of the constituents in the films. In turn, Nisin-Z's incorporation in the MC films was confirmed in Figure 1c,d. Furthermore, the requirements of good distribution and dispersion of Nisin-Z in the polymer matrix are met with these characteristics being critical in achieving homogeneity of antibacterial activity for food safety applications.

The solid surface affinity by water and air can be measured through the contact angle (θ), quantifying the hydrophobicity degree of films. The contact angle results and their respective regression curves are shown in Figure 2a. These results indicate that the concentration of LiCl or MgCl₂ modulated the contact angle. Incorporating different MgCl₂ concentrations (IS \geq 250 mM) changed the films' surface from hydrophilic to hydrophobic character, i.e., $\theta > 90^\circ$. According to Silva et al. [3], one of the reasons for the films' hydrophobicity increase is the unavailability of the MC's hydroxyl groups to interact with the water molecules localized on the film's surface.

In addition, the EC effect also influenced the contact angles' results. The behavior of films incorporated which Mg (⁺²) can be described by a quadratic regression while Li (⁺¹) by linear regression. These observations are justified by the change in the balance of the interfacial tension measurements between the film's surface, the drop of water, and the atmospheric air. There was likely an increase in the interfacial tension between the water drop and the films' surface. Salts diffused to the water drop, which caused a structural rearrangement of the water molecules through new interactions, e.g., ion-dipole, increasing hydrophobicity of the films.

3.2. WVP and Light Barrier Property

The incorporation of LiCl or MgCl₂ into polymeric dispersions, modulating their IS, caused a reduction of the WVP barrier of MC films. According to Kalkan et al. [26], one of the main factors influencing WVP water molecules' permeation and solubilization-diffusion effect. Thus, the water absorption (solvation) incremented with the IS increase since the presence of counterions (Li⁺¹ or Mg⁺²) changed the polarization affinity increasing the solubility of water from the external environment to the films, thus reducing WVP. Therefore, the IS of polymeric dispersions is remarkably capable of controlling WVP in MC films, achieving greater water vapor protection than other conventional plastics (EVOH, PET) or from renewable sources (bacterial cellulose, chitosan). Atta et al. [15], showed that incorporating yeasts into polymeric films reduces the equilibrium moisture due to the favoring of mass transfer. Therefore, combining these factors (incorporation of microorganisms and IS) can potentially modulate the WVP and other physicochemical properties of films for food packaging applications.

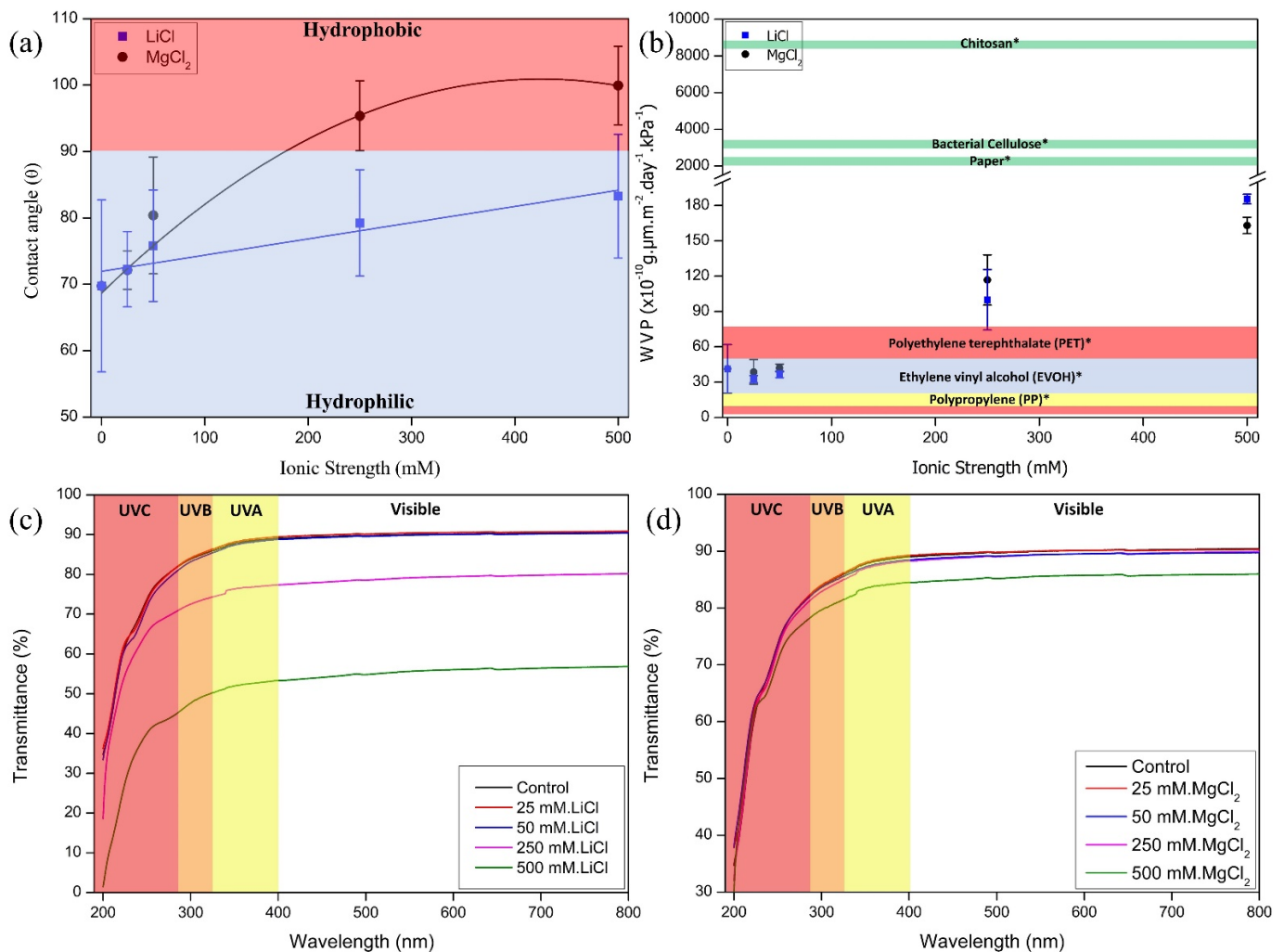


Figure 2. Contact angle (θ) measurement results between water and the surface of MC-based films with 0, 25, 50, 250 or 500 mM due to LiCl (a) or MgCl₂ (b) addition (the obtained models are presented in the Supplementary Materials). WVP results from MC-based films with 0, 25, 50, 250, and 500 mM due to LiCl or MgCl₂ addition and other conventional commodity plastics (PET, PP, and EVOH) and other films from renewable sources (Chitosan, bacterial cellulose, and paper) (b). The transmittance of MC-based films with 0, 25, 50, 250, and 500 mM due to LiCl (c) or MgCl₂ addition (d). Photographs of the films are shown in Figure S1 of the Supplementary Materials. * WVP values of conventional and renewable source films according to Wang et al. [27].

Polymeric films must be flexible and elastic to be used as a material for food packaging. Moreover, films must also guarantee the quality and safety of the food during storage. Therefore, films with UV–Vis radiation blocking can improve food preservation, minimizing photooxidation and photodegradation, especially in oils [28] and meat products [29]. Figure 2c,d exhibits the transmittance spectrum of films with added LiCl or MgCl₂. The ability to suppress UV–Vis radiation depends on the salt type (LiCl or MgCl₂) since they presented different results for films with the same IS and similar thickness (Table 1). For the same IS, the incorporation of LiCl into the MC matrices blocked more UV–Vis light than films with MgCl₂. Freitas et al. [25] demonstrated that films incorporated with ethanolic cabbage extract highlight another way to protect food against UV–Vis radiation. However, these additives, e.g., phenolic compounds and anthocyanins, are highly sensitive to visible light and reduce the protection capacity over time. Therefore, we show here that both salts are better options due to their stability over time and their ability to modulate the barrier

against UV–Vis light which can be achieved simply by adjusting the desired concentration to block the radiation.

Table 1. Mechanical performance, namely thickness (Tck), tensile strength (TS), Young’s modulus (YM), linear strain (ϵ_1) and density (D) of the MC-based films prepared at different IS (0; 25; 50; 250 and 500 mM) due to LiCl or MgCl₂ addition.

Treatment	Tck (mm)	TS (mPa)	YM (mPa)	ϵ_1 (%)	D (g·mL ⁻¹)
Control	73.1 (11) ^c	46.7 (7.3) ^a	1090.9 (42) ^a	41.3 (2.5) ^{bc}	1.14 (0.1) ^e
25 mM-LiCl	81.1 (6.5) ^c	25.0 (2.9) ^{bc}	629.3 (140) ^b	46.9 (8.4) ^{bc}	1.39 (0.1) ^d
50 mM-LiCl	97.7 (12.1) ^c	20.4 (4.7) ^c	219.5 (46) ^c	56.6 (13) ^b	1.40 (0.1) ^d
250 mM-LiCl	156.2 (7.4) ^b	7.0 (0.4) ^d	4.1 (0.6) ^d	134.9 (2.4) ^a	2.40 (0.2) ^b
500 mM-LiCl	251.5 (2.4) ^a	1.6 (0.3) ^d	1.6 (0.2) ^d	116.1 (9.5) ^a	4.25 (0.2) ^a
25 mM-MgCl ₂	81.3 (1.5) ^c	31.6 (4.0) ^{bc}	703.2 (189) ^b	38.3 (14.2) ^c	1.35 (0.1) ^d
50 mM-MgCl ₂	94.2 (8.2) ^c	38.8 (6.5) ^b	618.2 (79) ^b	46.0 (4.2) ^{bc}	1.40 (0.2) ^d
250 mM-MgCl ₂	164.6 (9.1) ^b	12.1 (0.9) ^d	13.6 (1.8) ^d	110.5 (6.7) ^a	1.75 (0.1) ^c
500 mM-MgCl ₂	249.3 (2.7) ^a	5.2 (0.3) ^d	3.7 (0.9) ^d	119.5 (11) ^a	2.17 (0.2) ^b

Means followed by the standard deviation between parentheses. Mean values followed by the same superscript letter within the same column are not significantly different according to Tukey’s test ($p > 0.05$).

3.3. Thermogravimetry and Moisture Content of Films

Thermal decomposition of MC-based films, with added LiCl or MgCl₂, were analyzed by thermogravimetry, and the curves were plotted as exhibited in Figure 3a–c. Three main events are highlighted, solvent evaporation (in blue), the decomposition of glycerol (in green), and the decomposition of MC (in red). It was observed that with the increase of salt concentration, the glycerol decomposition range and onset of the MC decomposition temperature reduced. This behavior can be attributed to the presence of the salts, which increase the physical spaces between polymeric chains, reducing the cohesive energy density of the interactions between MC-MC and MC-Glycerol [3,30]. Furthermore, a significant increase in water molecules into the polymeric matrix (i.e., equilibrium moisture content) occurred with increasing IS (Figure 3d). In this way, MC backbone scission reactions were catalyzed by hydrolysis, breaking skeletal bonds and reducing the MC decomposition temperature [3,31]. Atta et al. [15], also verified the reduction of the thermal stability of films based on bacterial cellulose due to the more significant amount of water molecules in the polymeric matrix resulting from the use of a hygroscopic plasticizer (glycerol).

In Figure 3d, it can be observed that the equilibrium moisture was similar for both salts (LiCl or MgCl₂) at the same level of IS. However, the decomposition rate of the MC-based film with Mg is significantly higher than the MC-based films with LiCl. This confirms EC as a factor that influenced the kinetics of the thermal decomposition of MC; however, complementary studies with counter-ions are being conducted to elucidate the cause of this effect. In any case, reducing thermal stability to 180 °C (500 mM corrected with MgCl₂) does not affect applications such as packaging for any food class. Therefore, the addition of chlorinated salts (or control of IS) remains a valid alternative for modulating the physicochemical properties of the films.

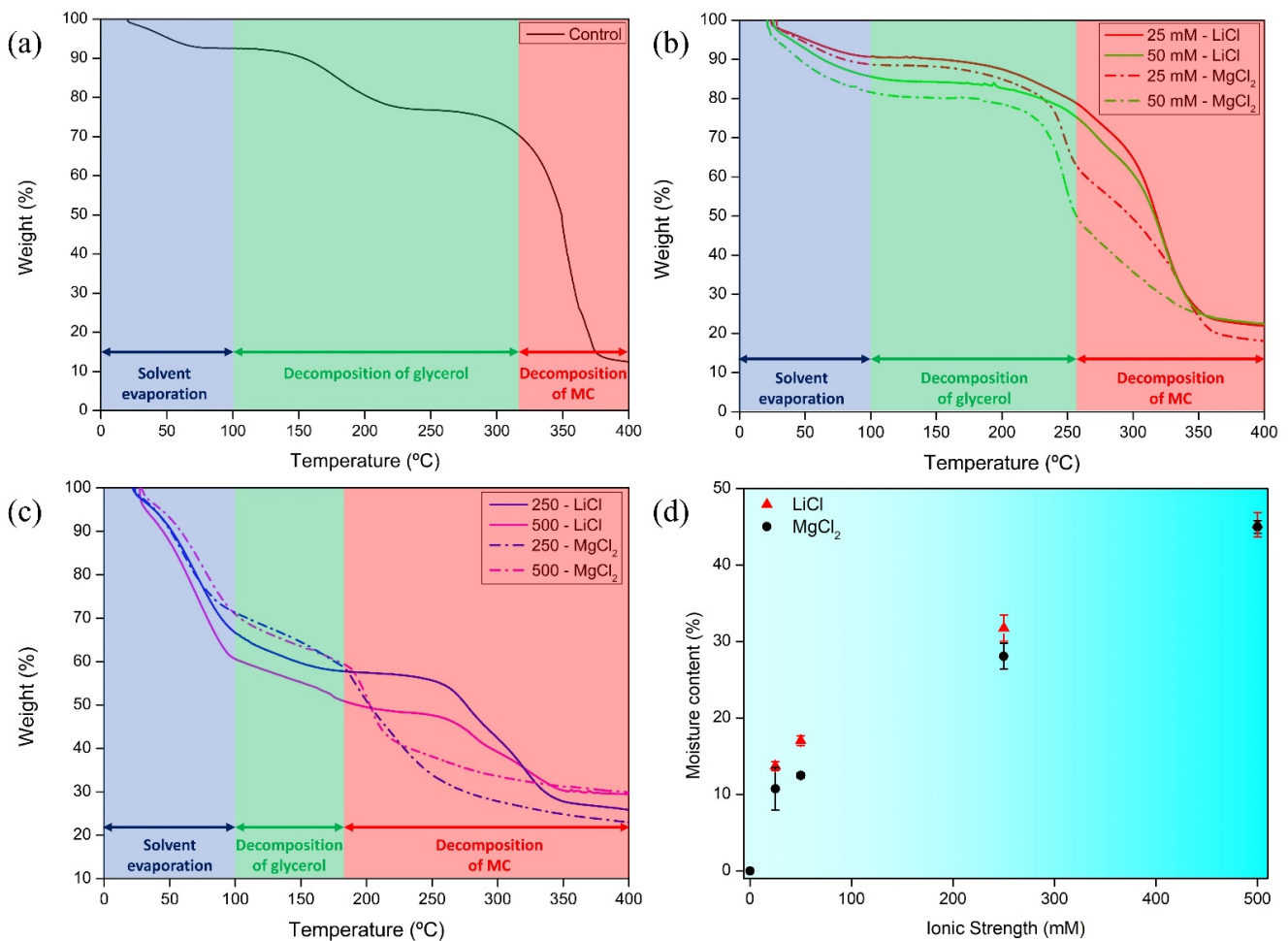


Figure 3. Thermal decomposition of MC-based films with 0 (a), 25, 50 (b) and 250, 500 mM (c) due to LiCl or MgCl₂ addition. Moisture content of the MC-based films prepared at different IS (0; 25; 50; 250, and 500 mM) corrected with addition of LiCl or MgCl₂ (d).

3.4. Density, Thickness, and Mechanical Performance

Among the main requirements for the development of bio-based films for food applications, elasticity and flexibility are important to wrap the product without generating damage or fractures of the film used as packaging, reducing the shelf life of the food. In this sense, new strategies to increase true strain and reduce Young's modulus have been developed using plasticizers [1,32], blends [33,34], and gamma irradiation [35]. Table 1 shows that the simple addition of chlorinated salts can modulate mechanical performance. In general, adding LiCl or MgCl₂ to MC-based films increased the thickness and EB, while YM and TM were reduced.

In general, the addition of LiCl or MgCl₂ to MC-based films increased Tck, ϵ_1 , and D, while YM and TM were reduced. These results can be explained by water absorption into the polymeric matrices due to the presence of the salts, as evidenced in the FTIR and moisture content results. The water in the polymeric matrix acted as a plasticizing agent, reducing the cohesive energy between the polymeric chains and providing greater flexibility and elasticity [31]. In turn, the increase in density of MC-based films was caused by the water filling of voids in the polymeric matrix. Thus, the density difference between MC-based films containing 500 mM LiCl versus MgCl₂ was the only significant difference from these results, comparing salts at the same IS level. Therefore, this behavior occurred due to greater LiCl mass added into the polymeric dispersion than MgCl₂ mass to achieve equivalence IS (as reported in the transmittance results).

In Figure 4a, the comparison between two methods of obtaining the strain of materials is shown, the true strain and the linear strain. We show here that up to 49% of errors can be obtained when the proper strain equation is not used, which unfortunately is a prevalent mistake in the literature [34,36–38]. In order to mitigate this problem, we show that the linear strain equation should be used when the maximum of up to 60% of strain (ϵ_f) is obtained concerning the initial specimen (ϵ_0). In turn, strains with values above 60% must use the true strain equation (also called logarithmic strain). We hope that this explanation contributes to reducing error propagation in the literature, the standardization of results and to serve as a validated reference for selecting suitable equations when calculating strain or percentage elongation. Figure 4b shows that the IS modulates the stiffness of MC-based films; that is, the greater the IS, the greater the flexibility. Thus, considering other conventional plastic applications in food, we confirm that an expansion of MC-based film applications can be achieved by IS modulation.

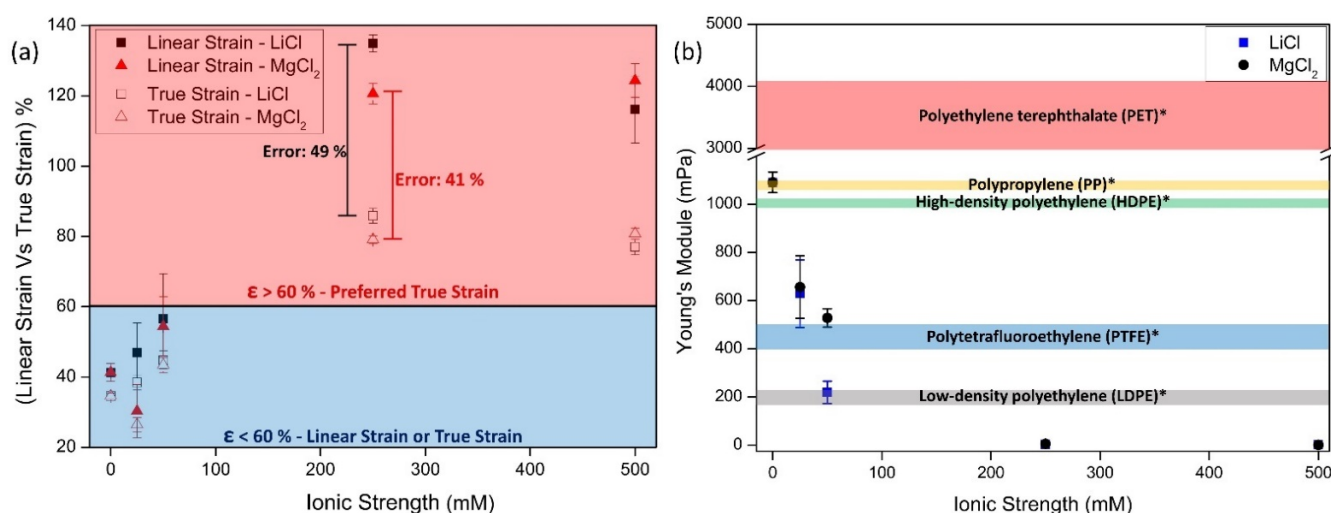


Figure 4. Linear Strain and True Strain results of MC-based films with IS of 0, 25, 50, 250, and 500 mM due to LiCl or MgCl₂ addition (a). YM results from MC-based films and other conventional commodity plastics (PET, PP, HDPE, LDPE, and PTFE) (b). * Young's modulus values of conventional plastics according to Callister and Rethwisch [39].

3.5. Antibacterial Activity

Nisin is a hydrophobic and cationic polypeptide produced by a number of strains of *Lactococcus lactis* subsp. *lactis* [40]. It is well known that nisin exerts antibacterial activity against a wide range of Gram-positive bacteria; on the other hand, its activity against Gram-negative bacteria, yeasts, and molds is primarily limited [41]. The higher resistance found for Gram-negative microorganisms could be related to the large size (1.8–4.6 kDa) of nisin, which restricts its passage across their outer membrane [11,42]. In parallel, the osmotic stress caused by lowering the water activity in the presence of solutes as salts (such as NaCl, LiCl, MgCl₂), sugar, or glycerol is well known [43].

The differences in susceptibility between Gram-positive and Gram-negative bacteria against nisin have been reinforced in the present study (Table 2). *E. coli*, a Gram-negative bacterium, only evidenced a discreet inhibition zone towards the film containing 500 mM of the monovalent salt (LiCl). However, considering the Gram-positive bacteria, *S. aureus*, and *L. plantarum*, even the control films produced exclusively with 10% Nisin-Z exhibited pronounced antibacterial activity. The respective inhibition zones can be observed in Figure 5. Previous studies mentioned that hydrophilic surfaces (e.g., methylcellulose matrix) enhanced both the release and water solubility of nisin, improving its antibacterial activity [44], which can explain the good properties of films against the target microorganisms.

Table 2. Inhibition zones (mm) of MC-films containing Nisin-Z and LiCl/MgCl₂ when evaluated against *S. aureus*, *L. plantarum* and *E. coli* on BHI solid media.

Treatment	Inhibition Zone (mm)		
	<i>S. aureus</i> (mm)	<i>L. plantarum</i> (mm)	<i>E. coli</i> (mm)
Control	21.7 (0.6) ^{ns}	15.7 (1.2) ^{bcd}	NA
25 mM-LiCl	20.6 (0.5) ^{ns}	14.2 (1.6) ^{cd}	NA
50 mM-LiCl	21.2 (0.3) ^{ns}	15.5 (0.8) ^{cd}	NA
250 mM-LiCl	20.1 (0.6) ^{ns}	16.3 (1.2) ^{abc}	NA
500 mM-LiCl	20.0 (0.4) ^{ns}	17.8 (1.3) ^{ab}	11.4 (0.5)
25 mM-MgCl ₂	21.1 (1.4) ^{ns}	14.5 (1.0) ^{cd}	NA
50 mM-MgCl ₂	21.7 (1.6) ^{ns}	13.8 (0.7) ^d	NA
250 mM-MgCl ₂	20.2 (0.3) ^{ns}	14.3 (1.9) ^{cd}	NA
500 mM-MgCl ₂	20.1 (0.6) ^{ns}	18.5 (0.6) ^a	NA

Average values were obtained, with three repetitions and standard deviation (SD). Non-significant (ns) at $p \leq 0.05$. NA: did not exhibit an inhibition zone. Mean values followed by the same superscript letter within the same column are not significantly different according to Tukey's test ($p > 0.05$).

Average values were obtained, with three repetitions and standard deviation (SD). Non-significant (ns) at $p \leq 0.05$. NA: did not exhibit an inhibition zone. Mean values followed by the same superscript letter within the same column are not significantly different according to Tukey's test ($p > 0.05$).

The activity exhibited by the film containing the maximum concentration tested of LiCl against *E. coli* contradicts results that mention the negative impact of a high concentration of salts (NaCl) on Nisin-Z activity [11]. This can be attributed to the fact that each salt can promote a different shift chance of amide N-H; intrinsically related to the nisin mechanism of action (i.e., the amide N-H protons of residues within two hydrophobic A and B rings at the N-terminus of Nisin-Z bind to the negatively charged pyrophosphate moiety of lipid II through a series of H-bond) [45–47]. Compared to Na⁺ from NaCl, Li⁺ is a strongly hydrated cation [47]. The hydration level of a cation will affect whether any observed chemical shift changes are a result of direct interactions of the cation with the peptide or adjustments to the peptide's hydration shell. Therefore, hydrated cations are less likely to interact with the large number of hydrophobic residues in Nisin-Z, reducing the reversal effect on the antibacterial properties of the peptide as provided by high concentrations of NaCl in previous studies [18]. In addition, the presence of LiCl on active films, by itself, may be responsible for an osmotic disbalance that influenced the susceptibility of *E. coli* to the film, developing synergism for antibacterial activity against Gram-negative bacteria.

No effect was observed for films containing 500 mM MgCl₂ against Gram-negative bacteria (Figure 5b). Despite Mg⁺² being known as a highly hydrated ion [46], the interference of this divalent cation on the inhibitory activity of antibacterial has been widely discussed. Thus, a hypothesis that supports the non-activity of films 500 mM-MgCl₂ against Gram-negative bacteria can be attributed to the fact that divalent cations are known to be crucial for the integrity of the bacterial outer membrane in these microorganisms. Indeed, chelation of divalent cations is a well-established method to permeabilize Gram-negative bacteria such as *E. coli*, allowing the inflow of hydrophobic antibacterial compounds [47]. Lipopolysaccharide constituents of the outer membrane of Gram-negative bacteria, are linked electrostatically via divalent cations (in particular, Mg⁺² and Ca⁺²), which bind to the anionic phosphate groups in the inner core, significantly contributing to resistance against hydrophobic antibacterial agents (e.g., nisin) [47,48]. Therefore, the presence of MgCl₂ reduced, even further, the permeability of nisin on the outer membrane of *E. coli*, reducing its activity, in comparison to the effect observed to the film added with LiCl.

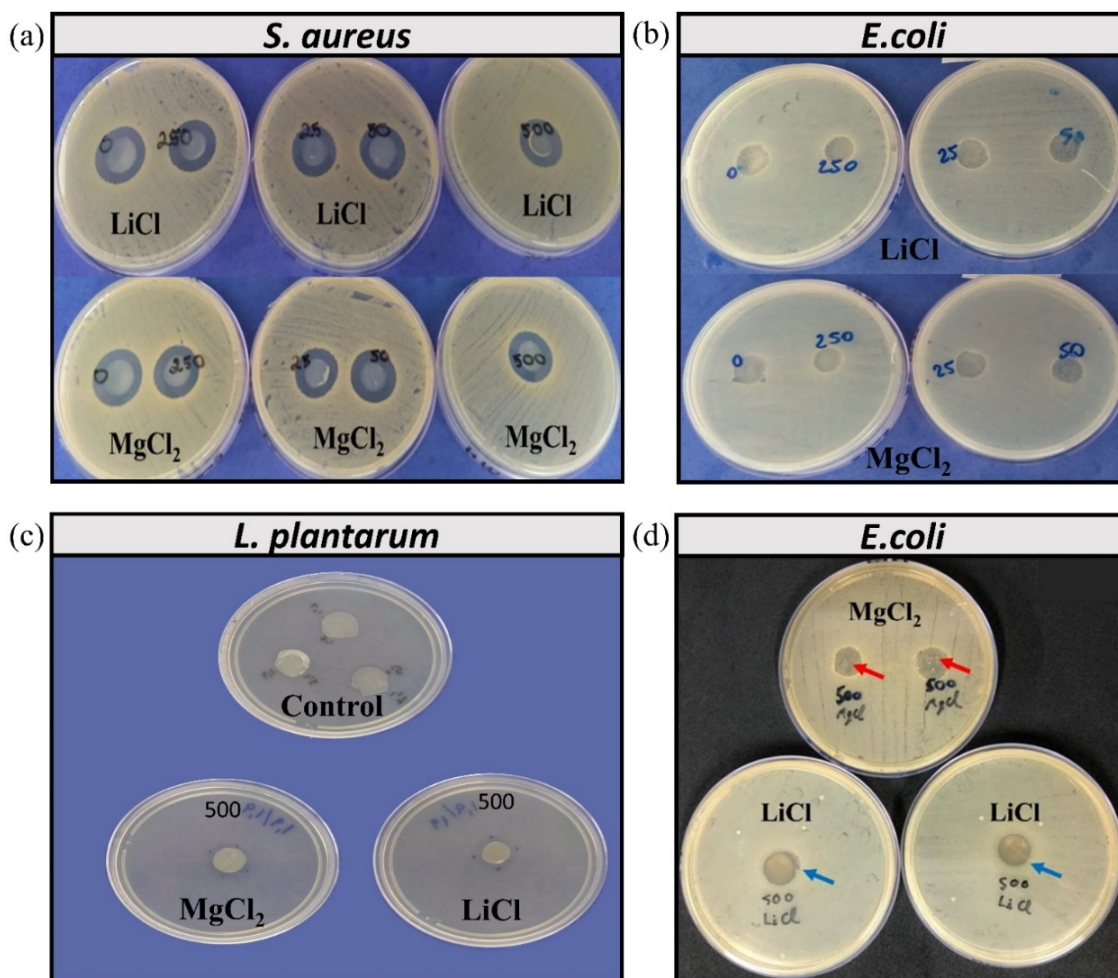


Figure 5. Photographs of the antibacterial activity of MC-based films with 10% of Nisin-Z with IS of 0, 25, 50, 250, and 500 mM due to LiCl or MgCl₂ addition, tested by direct contact against *S. aureus* (a) = tested at 37 °C/24 h. Photographs of the antibacterial activity of MC-based films with 10% Nisin-Z with IS of 0, 25, 50, and 250 mM (b) and 500 mM (d) due to LiCl or MgCl₂ addition, tested by direct contact against *E. coli*. Susceptibility of *L. plantarum* against the active films with IS of 0 (control) and 500 mM due to LiCl and MgCl₂ addition at 37 °C/48 h, under anaerobic conditions (c).

On the other hand, some studies have demonstrated the antibacterial potential of magnesium ions [49], which can also be observed on films prepared in the present study against the Gram-positive bacteria (Figure 5a,c). In corroboration to the ion hydration mentioned above, MgCl₂ and LiCl did not have a reversed nisin effect against *S. aureus* and *L. plantarum*. For these bacteria, all treatments (including control) evidenced an inhibition zone, highlighting the antibacterial effect of nisin. Regarding *S. aureus*, the type of salt and IS did not exert a significant effect on the antibacterial properties of the films ($p > 0.05$). Meanwhile, for *L. plantarum*, the 500 mM-MgCl₂ films presented the highest inhibition zone ($p \leq 0.05$). Other films, including 500 mM-LiCl, evidenced antibacterial activity similar to the control. Since the MgCl₂ in aqueous solution bears three ions in comparison to the two provided by LiCl, there is an enhanced osmotic pressure attributed to the divalent salt.

In this case, since Gram-positive bacteria do not present an outer membrane, the influence of MgCl₂ is different from the observed in *E. coli*. In addition to their presence on the outer membrane of Gram-negative bacteria, Mg is an important element to bacterial cells, and the intracellular concentration of Mg in many cell types is very high, ranging between 15 and 30 mM; thus, to exert osmotic stress on cells, it must be present in a concentration higher than this [50–53]. Both *S. aureus* and *L. plantarum* are halotolerant

microorganisms, tolerating higher concentrations of solutes than many other bacteria and likely require even higher amounts of salts to provide osmotic stress. However, the high amount of $MgCl_2$ on films prepared at 500 mM can be responsible for the extra antibacterial activity against *L. plantarum*.

4. Conclusions

In summary, the IS effect was studied by incorporating salts ($LiCl$ or $MgCl_2$) into MC polymeric dispersions. It was observed that the produced films exhibited higher equilibrium moisture content, reaching up to 50% by weight. Moreover, the water molecules acted as a plasticizing agent, modulating the MC's physicochemical properties. Furthermore, the incorporation of $MgCl_2$ at 500 mM of IS, obtained films with a hydrophobic surface ($\theta = 98^\circ$), stretchability (80%), and flexibility (3.7 MPa). In turn, with $LiCl$ incorporation into MC polymeric dispersions, films were produced with high elasticity and flexibility, better UV–Vis radiation block, and improved by synergism in the antibacterial activity against *E. coli*. Thus, we validated a new strategy to catalyze activity against Gram-negative bacteria using active films with Nisin-Z, extending protection against biological hazards in foods. In addition, we clarify the most appropriate method to determine the percentage elongation of films, aiming to mitigate frequent errors in the literature. Finally, we confirm that IS represents a new approach to bringing MC-based film properties closer to those of conventional plastics used in food applications.

Supplementary Materials: The following supporting information can be downloaded at: <https://www.mdpi.com/article/10.3390/polysaccharides3020026/s1>, Table S1: Adjusted regression equations, lack of fit values (LF), and coefficients of determination adjusted (R^2_{aj}) for contact angle of MC-based films added with $LiCl$ or $MgCl_2$ resulting in IS of 0, 25, 50, 250, or 500 mM. Figure S1: Photographs of MC-based films with IS of 0 (A, a) or 500 mM corrected for the addition of $LiCl$ (B, b) or $MgCl_2$ (C, c).

Author Contributions: Conceptualization, R.R.A.S. and N.d.F.F.S.; methodology, R.R.A.S., C.S.M. and N.d.F.F.S.; validation, R.R.A.S., C.S.M., T.R.A. and S.C.T.; formal analysis, R.R.A.S., C.S.M. and T.R.A.; investigation, R.R.A.S., C.S.M., T.R.A., S.C.T. and S.C.T.; resources, N.d.F.F.S., P.C.S. and A.C.d.S.P.; writing—original draft preparation, R.R.A.S., C.S.M. and T.R.A.; writing—review and editing, R.R.A.S., and T.V.d.O.; supervision, N.d.F.F.S., P.C.S. and A.C.d.S.P.; project administration, N.d.F.F.S.; funding acquisition, N.d.F.F.S. All authors have read and agreed to the published version of the manuscript.

Funding: This research was funded by National Council for Scientific and Technological Development (CNPq, grant number: 160448/2018-2). This study was also financed in part by the Coordenação de Aperfeiçoamento de Pessoal de Nível Superior-Brasil (CAPES)—Finance code 001.

Institutional Review Board Statement: Not applicable.

Informed Consent Statement: Not applicable.

Data Availability Statement: Not applicable.

Acknowledgments: The authors are grateful to the colleagues from the Food Packaging Laboratory of the Federal University of Viçosa (UFV) for exchanging experiences and knowledge.

Conflicts of Interest: The authors declare no conflict of interest.

References

1. Teixeira, S.C.; Silva, R.R.A.; de Oliveira, T.V.; Stringheta, P.C.; Pinto, M.R.M.R.; Soares, N.d.F.F. Glycerol and Triethyl Citrate Plasticizer Effects on Molecular, Thermal, Mechanical, and Barrier Properties of Cellulose Acetate Films. *Food Biosci.* **2021**, *42*, 101202. [CrossRef]
2. Aytac, Z.; Huang, R.; Vaze, N.; Xu, T.; Eitzer, B.D.; Krol, W.; MacQueen, L.A.; Chang, H.; Bousfield, D.W.; Chan-Park, M.B.; et al. Development of Biodegradable and Antimicrobial Electrospun Zein Fibers for Food Packaging. *ACS Sustain. Chem. Eng.* **2020**, *8*, 15354–15365. [CrossRef]

3. Silva, R.R.A.; de Freitas, P.A.V.; Teixeira, S.C.; de Oliveira, T.V.; Marques, C.S.; Stringheta, P.C.; dos Santos Pires, A.C.; Ferreira, S.O.; Soares, N.D.F.F. Plasticizer Effect and Ionic Cross-Linking: The Impact of Incorporating Divalent Salts in Methylcellulose Films for Colorimetric Detection of Volatile Ammonia. *Food Biophys.* **2021**, *17*, 59–74. [[CrossRef](#)]
4. Reichert, C.L.; Bugnicourt, E.; Coltelli, M.B.; Cinelli, P.; Lazzeri, A.; Canesi, I.; Braca, F.; Martínez, B.M.; Alonso, R.; Agostinis, L.; et al. Bio-Based Packaging: Materials, Modifications, Industrial Applications and Sustainability. *Polymers* **2020**, *12*, 1558. [[CrossRef](#)] [[PubMed](#)]
5. Moreirinha, C.; Vilela, C.; Silva, N.H.C.S.; Pinto, R.J.B.; Almeida, A.; Rocha, M.A.M.; Coelho, E.; Coimbra, M.A.; Silvestre, A.J.D.; Freire, C.S.R. Antioxidant and Antimicrobial Films Based on Brewers Spent Grain Arabinoxylans, Nanocellulose and Feruloylated Compounds for Active Packaging. *Food Hydrocoll.* **2020**, *108*, 105836. [[CrossRef](#)]
6. Wu, F.; Misra, M.; Mohanty, A.K. Challenges and New Opportunities on Barrier Performance of Biodegradable Polymers for Sustainable Packaging. *Prog. Polym. Sci.* **2021**, *117*, 101395. [[CrossRef](#)]
7. Freitas, P.A.V.; Siiva, R.R.A.; de Oliveira, T.V.; Soares, R.R.A.; Soares, N.F.F. Biodegradable Film Development by Nisin Z Addition into Hydroxypropylmethylcellulose Matrix for Mozzarella Cheese Preservation. *Int. J. Food Stud.* **2020**, *9*, 360–372. [[CrossRef](#)]
8. Fialho e Moraes, A.R.; Pola, C.C.; Bilck, A.P.; Yamashita, F.; Tronto, J.; Medeiros, E.A.A.; Soares, N.d.F.F. Starch, Cellulose Acetate and Polyester Biodegradable Sheets: Effect of Composition and Processing Conditions. *Mater. Sci. Eng. C* **2017**, *78*, 932–941. [[CrossRef](#)]
9. Yan, N.; Capezzuto, F.; Lavorgna, M.; Buonocore, G.G.; Tescione, F.; Xia, H.; Ambrosio, L. Borate Cross-Linked Graphene Oxide-Chitosan as Robust and High Gas Barrier Films. *Nanoscale* **2016**, *8*, 10783–10791. [[CrossRef](#)]
10. Caner, C.; Hernandez, R.J.; Harte, B.R. High-Pressure Processing Effects on the Mechanical, Barrier and Mass Transfer Properties of Food Packaging Flexible Structures: A Critical Review. *Packag. Technol. Sci.* **2004**, *17*, 23–29. [[CrossRef](#)]
11. Kuwano, K.; Tanaka, N.; Shimizu, T.; Nagatoshi, K.; Nou, S.; Sonomoto, K. Dual Antibacterial Mechanisms of Nisin Z against Gram-Positive and Gram-Negative Bacteria. *Int. J. Antimicrob. Agents* **2005**, *26*, 396–402. [[CrossRef](#)] [[PubMed](#)]
12. de Oliveira, T.V.; de Freitas, P.A.V.; Pola, C.C.; da Silva, J.O.R.; Diaz, L.D.A.; Ferreira, S.O.; Soares, N.d.F.F. Development and Optimization of Antimicrobial Active Films Produced with a Reinforced and Compatibilized Biodegradable Polymers. *Food Packag. Shelf Life* **2020**, *24*, 100459. [[CrossRef](#)]
13. Wang, H.; Liu, H.; Chu, C.; She, Y.; Jiang, S.; Zhai, L.; Jiang, S.; Li, X. Diffusion and Antibacterial Properties of Nisin-Loaded Chitosan/Poly (L-Lactic Acid) Towards Development of Active Food Packaging Film. *Food Bioprocess Technol.* **2015**, *8*, 1657–1667. [[CrossRef](#)]
14. Otoni, C.G.; de Moura, M.R.; Aouada, F.A.; Camilloto, G.P.; Cruz, R.S.; Lorevice, M.V.; Soares, N.d.F.F.; Mattoso, L.H.C. Antimicrobial and Physical-Mechanical Properties of Pectin/Papaya Puree/Cinnamaldehyde Nanoemulsion Edible Composite Films. *Food Hydrocoll.* **2014**, *41*, 188–194. [[CrossRef](#)]
15. Atta, O.M.; Manan, S.; Ahmed, A.A.Q.; Awad, M.F.; Ul-Islam, M.; Subhan, F.; Ullah, M.W.; Yang, G. Development and Characterization of Yeast-Incorporated Antimicrobial Cellulose Biofilms for Edible Food Packaging Application. *Polymers* **2021**, *13*, 2310. [[CrossRef](#)]
16. Atta, O.M.; Manan, S.; Shahzad, A.; Ul-Islam, M.; Ullah, M.W.; Yang, G.A. Biobased Materials for Active Food Packaging: A Review. *Food Hydrocoll.* **2022**, *125*, 107419. [[CrossRef](#)]
17. Ibarra-Sánchez, L.A.; El-Haddad, N.; Mahmoud, D.; Miller, M.J.; Karam, L. Invited Review: Advances in Nisin Use for Preservation of Dairy Products. *J. Dairy Sci.* **2020**, *103*, 2041–2052. [[CrossRef](#)]
18. Travers, W.; Kelleher, F. Studies of the Highly Potent Lantibiotic Peptide Nisin Z in Aqueous Solutions of Salts and Biological Buffer Components. *Biophys. Chem.* **2021**, *274*, 106603. [[CrossRef](#)]
19. ASTM D644-99; Standard Test Method for Moisture Content of Paper and Paperboard by Oven Drying. ASTM, American Society for Testing and Materials, ATSM: West Conshohocken, PA, USA, 1999.
20. ASTM D882-12; Standard Test Method for Tensile Properties of Thin Plastic Sheeting. ASTM, American Society for Testing and Materials, ATSM: West Conshohocken, PA, USA, 2012.
21. ASTM E96/E96M-10; Standard Test Method for Water Vapor Transmission of Materials. ASTM, American Society for Testing and Materials, ATSM: West Conshohocken, PA, USA, 2010.
22. M02-A12; Performance Standards for Antimicrobial Disk Susceptibility Tests; Approved Standard—Twelfth Edition. Clinical and Laboratory Standards Institute, CLSI: Filadelfia, PA, USA, 2015.
23. Tavares, A.G.; Andrade, J.; Silva, R.R.A.; Marques, C.S.; da Silva, J.O.R.; Vanetti, M.C.D.; de Melo, N.R.; Soares, N.D.F.F. Carvacrol-Loaded Liposome Suspension: Optimization, Characterization and Incorporation into Poly(Vinyl Alcohol) Films. *Food Funct.* **2021**, *12*, 6549–6557. [[CrossRef](#)]
24. Barbosa, L.C.A. *Espectroscopia No Infravermelho Na Caracterização de Compostos Orgânicos*, 1st ed.; Editora UFV: Viçosa, Brazil, 2007; Volume 1, ISBN 978-85-7269-280-9.
25. Freitas, P.A.V.; Silva, R.R.A.; de Oliveira, T.V.; Soares, R.R.A.; Junior, N.S.; Moraes, A.R.F.; Pires, A.C.D.S.; Soares, N.F.F. Development and Characterization of Intelligent Cellulose Acetate-Based Films Using Red Cabbage Extract for Visual Detection of Volatile Bases. *LWT* **2020**, *132*, 109780. [[CrossRef](#)]
26. Kalkan, S.; Otağ, M.R.; Engin, M.S. Physicochemical and Bioactive Properties of Edible Methylcellulose Films Containing Rheum Ribes, L. Extract. *Food Chem.* **2020**, *307*, 125524. [[CrossRef](#)]

27. Wang, J.; Gardner, D.J.; Stark, N.M.; Bousfield, D.W.; Tajvidi, M.; Cai, Z. Moisture and Oxygen Barrier Properties of Cellulose Nanomaterial-Based Films. *ACS Sustain. Chem. Eng.* **2018**, *6*, 49–70. [[CrossRef](#)]
28. Taoudiat, A.; Djenane, D.; Ferhat, Z.; Spigno, G. The Effect of *Laurus Nobilis*, L. Essential Oil and Different Packaging Systems on the Photo-Oxidative Stability of Chemlal Extra-Virgin Olive Oil. *J. Food Sci. Technol.* **2018**, *55*, 4212–4222. [[CrossRef](#)]
29. Boselli, E.; Rodriguez-Estrada, M.T.; Ferioli, F.; Caboni, M.F.; Lercker, G. Cholesterol Photosensitised Oxidation of Horse Meat Slices Stored under Different Packaging Films. *Meat Sci.* **2010**, *85*, 500–505. [[CrossRef](#)]
30. Canevarolo, S.V.J. *Ciência dos Polímeros. Um Texto Básico Para Tecnólogos e Engenheiros*; Artliber: São Paulo, Brazil, 2002; p. 280.
31. Freitas, P.A.V.; de Oliveira, T.V.; Silva, R.R.A.; e Moraes, A.R.F.; Pires, A.C.D.S.; Soares, R.R.A.; Junior, N.S.; Soares, N.F.F. Effect of PH on the Intelligent Film-Forming Solutions Produced with Red Cabbage Extract and Hydroxypropylmethylcellulose. *Food Packag. Shelf Life* **2020**, *26*, 100604. [[CrossRef](#)]
32. Kwon, C.W.; Chang, P.S. Influence of Alkyl Chain Length on the Action of Acetylated Monoglycerides as Plasticizers for Poly (Vinyl Chloride) Food Packaging Film. *Food Packag. Shelf Life* **2021**, *27*, 100619. [[CrossRef](#)]
33. De Oliveira, T.V.; de Freitas, P.A.V.; Pola, C.C.; Terra, L.R.; da Silva, J.O.R.; Badaró, A.T.; Junior, N.S.; de Oliveira, M.M.; Silva, R.R.A.; Soares, N.d.F.F. The Influence of Intermolecular Interactions between Maleic Anhydride, Cellulose Nanocrystal, and Nisin-Z on the Structural, Thermal, and Antimicrobial Properties of Starch-PVA Plasticized Matrix. *Polysaccharides* **2021**, *2*, 40. [[CrossRef](#)]
34. Wu, Z.; Huang, Y.; Xiao, L.; Lin, D.; Yang, Y.; Wang, H.; Yang, Y.; Wu, D.; Chen, H.; Zhang, Q.; et al. Physical Properties and Structural Characterization of Starch/Polyvinyl Alcohol/Graphene Oxide Composite Films. *Int. J. Biol. Macromol.* **2019**, *123*, 569–575. [[CrossRef](#)]
35. Bartolomei, S.S.; Santana, J.G.; Valenzuela Díaz, F.R.; Kavakli, P.A.; Guven, O.; Moura, E.A.B. Investigation of the Effect of Titanium Dioxide and Clay Grafted with Glycidyl Methacrylate by Gamma Radiation on the Properties of EVA Flexible Films. *Radiat. Phys. Chem.* **2020**, *169*, 107973. [[CrossRef](#)]
36. Prateepchanachai, S.; Thakhiew, W.; Devahastin, S.; Soponronnarit, S. Mechanical Properties Improvement of Chitosan Films via the Use of Plasticizer, Charge Modifying Agent and Film Solution Homogenization. *Carbohydr. Polym.* **2017**, *174*, 253–261. [[CrossRef](#)]
37. Lim, H.; Hoag, S.W. Plasticizer Effects on Physical-Mechanical Properties of Solvent Cast Soluplus®Films. *AAPS PharmSciTech* **2013**, *14*, 903–910. [[CrossRef](#)] [[PubMed](#)]
38. Pan, H.; Jiang, B.; Chen, J.; Jin, Z. Blend-Modification of Soy Protein/Lauric Acid Edible Films Using Polysaccharides. *Food Chem.* **2014**, *151*, 1–6. [[CrossRef](#)] [[PubMed](#)]
39. Callister, W.D., Jr.; Rethwisch, D.G. *Materials Science & Engineering—An Introduction*, 8th ed.; John Wiley & Sons, Inc.: Hoboken, NJ, USA, 2009; p. 721.
40. Irkin, R.; Esmer, O.K. Novel Food Packaging Systems with Natural Antimicrobial Agents. *J. Food Sci. Technol.* **2015**, *52*, 6095–6111. [[CrossRef](#)]
41. Remedio, L.N.; Silva dos Santos, J.W.; Vieira Maciel, V.B.; Yoshida, C.M.P.; de Carvalho, R.A. Characterization of Active Chitosan Films as a Vehicle of Potassium Sorbate or Nisin Antimicrobial Agents. *Food Hydrocoll.* **2019**, *87*, 830–838. [[CrossRef](#)]
42. Helander, I.M.; Mattila-Sandholm, T. Permeability Barrier of the Gram-Negative Bacterial Outer Membrane with Special Reference to Nisin. *Int. J. Food Microbiol.* **2000**, *60*, 153–161. [[CrossRef](#)]
43. Sperber, W.H. Influence of Water Activity on Foodborne Bacteria-A Review. *J. Food. Prot.* **1983**, *46*, 142–150. [[CrossRef](#)]
44. Zimet, P.; Mombrú, Á.W.; Castro, A.; Villanueva, J.P.; Pardo, H.; Rufo, C. Physico-Chemical and Antilisterial Properties of Nisin-Incorporated Chitosan/Carboxymethyl Chitosan Films. *Carbohydr. Polym.* **2019**, *219*, 334–343. [[CrossRef](#)]
45. Panina, I.; Krylov, N.; Nolde, D.; Efremov, R.; Chugunov, A. Environmental and Dynamic Effects Explain How Nisin Captures Membrane-Bound Lipid II. *Sci. Rep.* **2020**, *10*, 8821. [[CrossRef](#)]
46. Hsu, S.T.D.; Breukink, E.; Tischenko, E.; Lutters, M.A.G.; de Kruijff, B.; Kaptein, R.; Bonvin, A.M.J.J.; van Nuland, N.A.J. The Nisin-Lipid II Complex Reveals a Pyrophosphate Cage That Provides a Blueprint for Novel Antibiotics. *Nat. Struct. Mol. Biol.* **2004**, *11*, 963–967. [[CrossRef](#)]
47. Collins, K.D.; Brauman, J.I. Sticky Ions in Biological Systems (Ion Hydration/Potassium Ion/Ammonium Ion/Protein Structure/Hofmeister Series). *Proc. Natl. Aca. Sci. USA* **1995**, *92*, 5553–5557. [[CrossRef](#)]
48. Rao, J.S.; Dinadayalane, T.C.; Leszczynski, J.; Sastry, G.N. Comprehensive Study on the Solvation of Mono- and Divalent Metal Cations: Li⁺, Na⁺, K⁺, Be²⁺, Mg²⁺ and Ca²⁺. *J. Phys. Chem. A* **2008**, *112*, 12944–12953. [[CrossRef](#)] [[PubMed](#)]
49. Clifton, L.A.; Skoda, M.W.A.; le Brun, A.P.; Ciesielski, F.; Kuzmenko, I.; Holt, S.A.; Lakey, J.H. Effect of Divalent Cation Removal on the Structure of Gram-Negative Bacterial Outer Membrane Models. *Langmuir* **2015**, *31*, 404–412. [[CrossRef](#)]
50. Schneck, E.; Schubert, T.; Konovalov, O.V.; Quinn, B.E.; Gutschmann, T.; Brandenburg, K.; Oliveira, R.G.; Pink, D.A.; Tanaka, M. Quantitative Determination of Ion Distributions in Bacterial Lipopolysaccharide Membranes by Grazing-Incidence X-Ray Fluorescence. *Proc. Natl. Acad. Sci. USA* **2010**, *107*, 9147–9151. [[CrossRef](#)]
51. Demishtein, K.; Reifen, R.; Shemesh, M. Antimicrobial Properties of Magnesium Open Opportunities to Develop Healthier Food. *Nutrients* **2019**, *11*, 2363. [[CrossRef](#)]
52. Lin, Z.; Sun, X.; Yang, H. The Role of Antibacterial Metallic Elements in Simultaneously Improving the Corrosion Resistance and Antibacterial Activity of Magnesium Alloys. *Mater. Des.* **2021**, *198*, 109350. [[CrossRef](#)]
53. Wolf, F.I.; Torsello, A.; Fasanella, S.; Cittadini, A. Cell Physiology of Magnesium. *Mol. Asp. Med.* **2003**, *24*, 11–26. [[CrossRef](#)]